Impact of climate variability on alpine glaciers in North-Western Italy

Sandro Calmanti

ENEA-CLIM Casaccia, Roma, Italy

Luigi Motta

Dip. Scienze della Terra, Università di Torino, Italy

Marco Turco

ARPA Piemonte, Torino, Italy

Antonello Provenzale

ISAC-CNR, Torino and CIMA, Savona, Italy

Keywords: Climate variability at regional scales, impact of climate change, hydrologic cycle in alpine areas, glacier dynamics.

Correspondence to:

Antonello Provenzale, ISAC-CNR, Torino, Corso Fiume 4, I-10133 Torino, Italy

Phone: + 39 011 3839833 , fax: + 39 011 6600364

email: a.provenzale@isac.cnr.it

Abstract

We analyze a large set of glacier snout fluctuation data in Piedmont and Val d'Aosta (Italy) and study the impact of climate variability on valley glaciers in the western Italian Alps. The study period includes about 70 y during the 20th Century; we focus on the last 50 y where a large number of temperature and precipitation time series are available. Superposed onto a general recession trend, we find strong oscillations on decadal time scales that are well correlated with fluctuations in winter precipitation rates and average summer temperatures. We construct a simple lagged-linear empirical stochastic model that explains up to 66% of the variance of the snout fluctuation data when summer temperature and winter precipitation are used as proxies for the glacier mass balance. This model produces reliable out-of-sample predictions of the average response of alpine glaciers to climate variability and it can be used to forecast glacier response in different climate change scenarios.

1. Introduction

Climate fluctuations on regional scales generally include a modification of the hydrologic cycle. In mid-latitude mountain areas, alpine-type glaciers are a central component of the local hydrologic budget; in addition, they are an important source of drinkable water and provide part of the supply to hydroelectric power plants. Episodes of mountain glacier retreat, as observed in many parts of the world, can cause instabilities of the mountain slopes and have the potential of generating flood events associated with the break-up of ice dams or frontal moraines (e.g., Clague and Evans, 2000, Kaser and Osmaston, 2001). Understanding and quantitatively predicting the response of alpine glaciers to climatic variability is thus both a challenging scientific issue and a practical task that needs to be addressed for planning purposes.

Alpine-type glaciers are often pictured as good climatic indicators, as they have only extremely weak, if any, feedback on the climate system (e.g., Haeberli, 1995, Oerlemans, 2001). The direct action of climate variability on glacier dynamics is effected by modifications in the annual net mass balance, $b_i = c_i - a_i$, where c_i is the accumulation rate in year i and a_i is the ablation rate (e.g., Paterson, 1994). When the net mass balance is positive, $c_i > a_i$, the mass of the glacier increases. When ablation dominates over accumulation, the net mass balance is negative and the glacier loses mass. In general, accumulation is maximum in winter, at the highest elevations on the glacier above the Equilibrium Line Altitude (ELA, defined as the line that marks the elevation where annual accumulation and ablation balance), and ablation is largest in summer, below the ELA. Fluctuations in the annual net mass balance generate variations in the glacier profile, that modify the ice flow pattern inside the glacier. This leads to modifications in the glacier length and in the position of the glacier terminus (or snout). Figure 1 shows a picture of the Pre de Bar glacier in Val d'Aosta (Italy), one of the glaciers considered here, with a schematic indication of the accumulation and ablation areas.

Oerlemans (2001) pictures mountain glaciers as brownian particles that are pushed around by irregular fluctuations of the equilibrium line altitude. However, the adjustment of a glacier to new climatic conditions is delayed in time, due to the slow glacier response to changes in the mass balance (Paterson, 1994). As a consequence, high-frequency climatic oscillation are low-pass filtered by the glacier, with a cut-off frequency that depends on the glacier's characteristics.

An abrupt climate switch between two distinct, steady climate regimes would thus result into a gradual approach of the glacier to a new steady state, rather than into a brisk step at the time of the transition.

Glaciers in the Western Alps show a widespread retreat, that started in the second half of the 19th century (Greene *et al*., 1999, Vannuzzo, 2001). This tendency is associated with climate change, and it is observed worldwide with just a few exceptions (e.g., Nesje, 1989, Theakstone, 1990, Yafeng and Jiawen, 1990, Harper, 1993, Holmlund and Fuenzalida, 1995, Chinn, 1996, Kaser, 1999, Harrison and Winchester, 2000, Nesje and Dahl, 2000, Vincent, 2002, Kaser *et al*., 2004), although climatic control is not the only mechanism of glacier advance and retreat (e.g., Sturm *et al*. 1991). The almost synchronous retreat of the world glaciers is documented by different kinds of measurements, ranging from mass balance data to ELA shifts, to glacier snout fluctuations. The Intergovernmental Panel for Climate Change, Working Group I, reports a "highly significant" correlation between the increase in Northern hemisphere land temperature and the decrease in land-ice extent. The shift of the ELA in the Alps has been used to estimate a temperature increase of 0.5 to 1.0 °C over the last Century (Pelfini, 1994, Vanuzzo, 2001), in agreement with the trend reported by the IPCC (0.6 ± 0.2 °C since the late 19th Century), with the results of a direct analysis of temperature variability in the European Alps (Bohm *et al*., 2001), and with the trends in the 20th Century in North-Western Italy (Ciccarelli *et al*., 2006).

The century-scale glacier retreat is modulated by fluctuations on shorter time scales, associated with climate variability on decadal time scales (e.g., Nesje and Dahl, 2000, Oerlemans 2001). In past studies, many types of empirical and/or dynamical models have been proposed to relate glacier mass balance and/or terminus advances and retreats to climatic variability (e.g., Posamentier, 1977, Kruss, 1984, Letreguilly, 1988, Laumann and Reeh, 1993, Oerlemans *et al*., 1998, Braithwaite and Zhang, 1999, Oerlemans and Reichert, 2000, Oerlemans, 2001, Van de Wal and Wild, 2001). In this work we focus on decadal glacier snout fluctuations and build a data-driven, empirical model that links the average variability of the terminus position of a set of mountain glaciers in the North-Western Italian Alps to winter precipitation rates and mean summer temperatures. The link is sought in the form of a lagged-linear stochastic model. Linearity in glacier fluctuation response is assumed as the simplest working hypothesis, which we verify in the course of the analysis. Following standard procedures (e.g., Tong 1990), we require the stochastic term in the model to be Gaussian and uncorrelated and we try to maximize

the variance explained by the deterministic part. We show that this simple model can be used to produce out-of-sample predictions of the average glaciers' response to climatic variability, and it could be nested into climate change scenarios produced by regional climate models (e.g., Giorgi and Mearns, 2002).

The rest of this paper is organized as follows: section 2 introduces the snout fluctuation data and the climatic data employed in this study. Section 3 is devoted to an empirical assessment of the sensitivity of alpine glaciers to climatic variables such as precipitation and temperature. Section 4 contains a discussion of the empirical model and of the statistical methods adopted to build and validate it. In section 5 we report the results of the modelling exercise. Section 6 addresses the issue of using the empirical model developed so far to provide out-of-sample predictions of the glacier response. A discussion of the results and some perspectives are reported in section 7.

2. Glacier and climate data

The estimate of glacier fluctuations on decadal time scales requires the availability of time series of glacier response and of climate variability on a sufficiently long period of time. This requirement forced us to use proxy data as a substitute for the quantitative measurement of glacier mass balance, which is generally available, at least for the area of our study, only for few glaciers and for limited periods of time. The validity of the choice of proxy data is assessed *a posteriori*, based on the ability of the empirical model to reproduce and predict the average glaciers' behavior.

2.1 Snout position data

In this study we focus on a set of selected glaciers from the Western sector of the Italian Alps, in the area of Piedmont and Val d'Aosta. Figure 2 shows a schematic map of the region under study, indicating the areas where glaciers are found. Glacier's snout data are collected by the staff of the *Comitato Glaciologico Italiano - Consiglio Nazionale delle Ricerche* (CGI-CNR) and regularly published on the CGI Bullettin (*Geografia Fisica e Dinamica Quaternaria*). All glaciers considered here are located inside a rectangular area having its North-Western corner at 46° 24' 30" N – 4° 07' 00" E and its South-Eastern corner at 44° 07' 00" N - 5° 38' 20" E. The whole data set can be divided into two subsets (reported in tables 1 and 2 respectively):

- G27-99: measurements from 1927 to 1999, 9 large glaciers (table 1);

- G69-99: measurements from 1969 to 1999, 45 glaciers including those in G27-99 (table 2).

< FIGURE 1 about here (picture of the Pre de Bar glacier) >

< FIGURE 2 about here: Map of glaciated areas >

< TABLE 1 about here: G27-99 >

< TABLE 2 about here: G69-99 >

The raw data are the distances, D_{ik}^{j} , $\left(k=1,...,M_{i}^{j}\right)$, between a set of M_{i}^{j} points at the snout of the *j*-th glacier and an ensemble of fixed landmarks. The index i represents the year of the measurement. The landmarks at the glacier snout are chosen by the observers on the basis of the glacier's conditions; landmarks can be changed from one year to another (keeping track of the difference between the new position and the old one) if the glacier's morphology undergoes relevant changes. The change of a landmark is a potential source of error as the relationship between new and old landmarks is not always recorded with high precision. In the analysis that follows, for each year and for each glacier we consider the mean glacier's snout position, X_{i}^{j}, calculated by averaging D_{ik}^{j} over the M_{i}^{j} measurements that are available on the *i*-th year. We then focus on the mean annual snout variation:

$$\delta X_{i}^{j}=X_{i}^{j}-X_{i-1}^{j} \tag{1}$$

which measures the change in the glacier's snout position from the previous to the current year. Note that δX_{i}^{j} can be computed only if both X_{i}^{j} and X_{i-1}^{j} are available: A gap of one year in the measurement of X_{i}^{j} implies a gap of two years in the time series of δX_{i}^{j}.

Sample time series of the annual terminus positions, X_i^j, for five glaciers in the set G27-99 are shown in figure 3. The corresponding time series of annual snout fluctuations are shown in figure 4. The longest time series comes from the Lys glacier. This glacier has been almost continuously monitored from 1913. All the glaciers shown in figure 3 underwent significant retreat during the measurement period. The retreat appears to be more rapid for the Lys, the Belvedere and the Pre de Bar glaciers, which are the largest glaciers in the data set. In particular, the Lys and Belvedere glaciers have retreated by almost 500 meters since 1930. In the early '60s, the Pre de Bar glacier entered an advancing phase, followed, with some delay, by other glaciers. The Pre de Bar and Lex Blanche glaciers seem to anticipate the onset of the advancing phase of Lys, consistent with the fact that the latter is considerably longer than the others. In the data set G69-99, only short and sparse time series are available, and individual records are not shown.

< FIGURE 3 about here (sample time series of glacier snout positions) >

< FIGURE 4 about here (sample time series of glacier snout fluctuations) >

Tables 1 and 2 provide, for each of the glaciers in the two data sets, the values of the average snout fluctuation, $\overline{\delta X^j}$, and of the r.m.s. deviation, σ^j. Almost all values of $\overline{\delta X^j}$ are negative, confirming the widespread retreat of Alpine glaciers in this area. However, the values of σ^j are usually larger than the average snout fluctuations, indicating the presence of strong variability superposed on the recessional trend. To compare and average the behavior of different glaciers, in all the following analyses we use the standardized snout fluctuations, δx_i^j, defined as

$$\delta x_i^j = \left[\delta X_i^j - \overline{\delta X^j}\right] \Big/ \sigma^j \quad . \tag{2}$$

2.2 Distribution of snout fluctuations

First we analyze the probability distributions of the standardized annual snout fluctuations, $p(\delta x_i^j)$, for the two data sets G27-99 and G69-99. Two different tests for Gaussianity are performed, namely the standard χ^2 and the Kolmogorv-Smirnov (KS) tests. The results reported in table 3 show that when the tests are performed on the entire data sets, the hypothesis that the snout fluctuations have a Gaussian PDF must be rejected. Visual inspection of the time series suggest that non-Gaussianity is due to the presence of sparse outliers. To explore this possibility, for each glacier we define as a potential outlier any snout fluctuation δX_i^j lying at a distance larger than $3\sigma^j$ from the mean fluctuation $\overline{\delta X^j}$. For each potential outlier, we search in the documentation available in the GCI bulletins to check whether unusual events were reported for that year. For the G27-99 data set, the documentation confirms that whenever a potential outlier is detected, either ice break-up, melting of a thin residual layer, or the presence of a lingering snow cover may have caused an anomalous estimate of the glacier snout position. However, no such relation could be established for the data set G69-99.

In the analysis that follows, we opted for removing the documented outliers from the G27-99 data set. Once these data points are discarded, the distribution of snout fluctuations becomes Gaussian, as indicated by the results of the KS and χ^2 tests reported in table 3. The Gaussianity of the snout fluctuations for the long data set G27-99 is interesting because it is consistent with the view that glacier snout fluctuations can be described as Brownian fluctuations driven by variations in climatic indices (Oerlemans 2001). The observed Gaussianity also indicates that a linear empirical model can be adopted, at least as a first step, to describe glacier snout fluctuations in G27-99. We note, anyway, that the deviation from Gaussianity is quite mild even when the whole G27-99 data set is retained, and the results reported in the following sections do not significantly change when all data points (including the outliers) are included in the analysis.

< TABLE 3 about here: tests for Gaussianity >

For the G69-99 data set the situation is more complicated, as no documentation justifies the exclusion of most of the potential outliers. A linear model is thus bound to provide poorer results for this data set. At present, we cannot offer a definite explanation on the origin of non-

Gaussianity of snout fluctuations in G69-99. We note, however, that this data set contains measurements from a range of glaciers with widely different size, orientation and characteristics, and the sample can hardly be considered to be homogeneous.

2.3 Average time series of snout fluctuations

Figure 5 shows the average (standardized) glacier snout fluctuations for the two data sets, together with the fraction of retreating glaciers in each year. The documented outliers were removed from data set G27-99, and the averaged time series have been further averaged by a 5-y running mean. The annual snout fluctuations averaged over G27-99 and G69-99 are consistent with each other, and an oscillation with approximately decadal time scale appears to be a robust feature of the averaged signals. The decadal oscillation in the snout fluctuation is anti-correlated with the fraction of retreating glaciers. This indicates that the oscillations around the recessional trend are not dominated by the behaviour of a few large glaciers but they represents the average, collective response of glaciers in the North-Western Italian Alps to fluctuations in climatic conditions on decadal time scales.

< FIGURE 5 about here: average glacier snout fluctuations >

2.4 Climatic Data

In past years, much work has been done on relating glacier mass balance to meteorological parameters, see e.g. Vincent (2002) and references therein for a study on four French glaciers. In general, these relationships are rather complicated and vary even on individual glaciers. Here, we are not trying to capture the details of the dynamic and thermodynamic processes affecting the response of individual glaciers. Rather, we seek for a quantitative estimate of the average response of an ensemble of glaciers to decadal climate variability.

With this objective in mind, we focus on the records of temperature and precipitation, which are available in the study area for the last 50 years (temperature) and 90 years (precipitation), and verify whether these can be used to estimate and predict glacier snout fluctuations. In the following, we use the data collected by the ground-based observational network managed by

ARPA Piemonte in North-Western Italy. We use the records of daily precipitation rates, P, and minimum and maximum temperatures, respectively $T_{\min}$ and $T_{\max}$, recorded by a large number of weather stations in Piedmont and Val d'Aosta. Since maximum and minimum temperatures are strongly correlated in this data set, the mean daily temperature $T = (T_{\max} - T_{\min})/2$ is used in the analysis. For each weather station, monthly averages are computed. Only months for which more than 20 days of observations are available are retained in the analysis.

An important point concerns the selection of the meteorological stations. The option of choosing, for each glacier, the meteorological measurements that are closer in space to the location of the glacier itself, turns out to be potentially misleading. In fact, not only weather stations are hardly found in close proximity of the glaciers but, most importantly, local variability could blur the regional climate signal. Another option, which is adopted here, is to average the meteorological records over a larger area to provide a mean regional climatic record. Since glaciers respond slowly to weather changes and integrate the climate forcing over time, we believe that looking at the average regional meteorological record is preferrable when considering the average response of the glaciers in an extended area.

Following this approach, we obtain a mean regional climatic time series by averaging over all measurement stations. In the analysis that follows, we always consider standardized variables, rather than raw values, to reduce bias due to differences in the altitude and position of the weather stations. Therefore, monthly averages for each station are first standardized by subtracting the mean and dividing by the r.m.s. fluctuation before averaging over different stations. The monthly data are then aggregated to provide seasonal values. In appendix 1 we give a brief account of the computation, step by step, of the average seasonal precipitation, $P_{i(n-m)}$, where *n* and *m* indicate the months marking the beginning and the end of the season and *i* labels the year. The same procedure is used to compute the seasonal temperature, $T_{i(n-m)}$.

3. Glacier response to climate variability

The seasonal cycle in the Western Alps is characterized by minimum temperatures in the months of December/January and maximum temperatures in July/August. Precipitation has an annual

cycle with maxima in spring (May) and fall (November) and minima in July and January (e.g., Regione Piemonte, 1998). The response of alpine glaciers to climate variability is mediated by the glacier mass balance, which depends on the difference between accumulation (mainly in winter) and ablation (mainly in summer). Here we make the working hypothesis that winter precipitation is a good proxy for accumulation. In general, only precipitation at temperatures below freezing should be taken into account (e.g., Vincent 2002). For most of the alpine glaciers considered here, however, winter precipitation falls as snow, and one can tentatively use the time series of winter precipitation. The definition of a proxy data set for summer ablation is more delicate. An important variable affecting ablation is summer insolation, whose record, however, is not available for the data set under study. As a proxy for ablation, we use the record of summer temperatures.

A first issue concerns the definition of the time lag between variations in temperature and precipitation and glacier snout fluctuations: Even though climatic variations induce rapid changes in the glacier mass balance, there is a time delay, τ, between a variation in mass balance and the corresponding fluctuation in the glacier snout position. Several order-of-magnitude estimates of the response time τ, based on different physical arguments, can be found in the literature. Paterson (1994) suggests $\tau = H/a$, where H is the maximum thickness of the glacier and a is the ablation rate at the terminus. Paterson's estimate, when applied to temperate glaciers in maritime climate such as those considered here, gives a response time of 10-60 y.

In the following we use an empirical approach, and we estimate the value of the time lag between meteo-climatic variables and glacier snout response, as well as the appropriate duration of the “winter” and “summer” seasons from the point of view of accumulation and ablation, by systematically examining the lagged cross-correlations between climatic variables and snout fluctuations. The ablation period is easily identified in the warmest, driest summer months, during which insolation is maximum. The duration of summer is estimated as the time period, centred around July-August, for which there is the largest negative lagged cross-correlation between glacier snout fluctuations and temperature. The accumulation period is assumed to be centred on December-January and its duration is estimated by maximizing the lagged correlation with precipitation. Different durations are considered and the corresponding lagged correlations are estimated for several different values of the time lag.

A confidence level for the lagged cross-correlation coefficient, $r(\tau)$ where τ is the time lag between either temperature or precipitation and snout fluctuations, can be estimated in a non-parametric way by employing a randomization technique (see also the discussion in section 4). In this test, one of the time series is kept fixed and the other (say the climatic variable) is randomly shuffled before estimating the correlation coefficient. In this way, the theoretically expected value for the cross correlation between snout fluctuations and the shuffled climatic variable is zero. The procedure is repeated many times and the fraction of trials which result in values of the correlation coefficients that are larger than the original one (in absolute value) is taken to represent the empirical probability that the estimated value of the correlation coefficient occurred by chance (see, e.g., Jacobson *et al*., 2004, and references therein). In addition to the randomization probability, an error bar, δr, can be associated with each value of r. This is done by a *jackknife* procedure in which we randomly select half of the data values from the entire time series and then compute the correlation coefficient from the selected subset. Again, the procedure is repeated many times and the values that bracket 95% of the correlation coefficient estimates can be taken as an estimate the error bars. If the error bars include zero, then the correlation is not significant.

The results on the lagged cross-correlations between climatic data and snout fluctuations are reported in tables 4-6. Only correlations with a confidence level of at least 95% (obtained from the random shuffling method) are shown.

< TABLE 4 about here: lagged cross-correlations >

< TABLE 5 about here: lagged cross-correlations >

< TABLE 6 about here: lagged cross-correlations >

3.1 Winter precipitation

When considering the full period (1927-1997), the cross-correlation between glacier fluctuations and precipitation is not very high (between 0.4 and 0.5) and the time lag is about 9 years. Figure

6 shows the average snout fluctuations for G27-99 together with a set of seasonal precipitation data, shifted by their maximum correlation time lag τ (see table 4). Around 1950 there is a sudden change in the phase between the two signals. We then computed the cross-correlation for the periods 1927-1950 and 1950-2000 separately (table 5). The average cross-correlation between precipitation and glacier response in the two separate halves increase significantly, reaching r=0.6 for the period 1927-1950 and almost r =0.8 for the period 1950-2000. In addition, the time lags in glacier response are different for the two periods, with a larger lag of about 9-10 years during the second half of the Century and a smaller lag of about 6 years during the first half. This suggests a change in the dynamical regime of the glaciers that took place at the middle of last Century. This interpretation is supported by the fact that after 1950 most glaciers entered a phase of slow advance (or slower retreat).

< FIGURE 6 about here: average snout fluctuations and average winter precipitation >

< FIGURE 7 about here: cross-correlation between snout fluctuations and winter precipitation >

In particular, after 1950, the average precipitation of the extended winter period, November to March, shows the highest cross-correlation with the mean annual snout variation (r=0.78), with lag τ = 10 y. Figure 7 shows the lagged cross-correlation between glacier snout fluctuations and winter precipitation (from November to March) as a function of the lag.

The seasonal precipitation data were also cross-correlated with the mean annual G69-99 snout fluctuations. All climate indices show lower correlation than with G27-99. Similarly to the case of G27-99, the largest correlation is found for the extended winter period, from November to March, though with a slightly shorter time lag.

3.2 Temperature

In the case of the temperature record, climate indices can be computed only for the second half of the last Century. Therefore, no comparison between the retreating and advancing phases is possible. Also in this case, several composites where systematically correlated with the mean

annual snout variation (table 6). Figure 8 shows the average snout fluctuations for G27-99 together with a set of seasonal temperature variables shifted by their maximum correlation time lag τ.

For the case of G27-99, the average correlation with the climatic indices is about r = 0.6, with time lags between 6 and 9 years. The index that shows the largest correlation (r = 0.63) corresponds to the extended summer period, from May to October, and to a time lag τ = 8 y. Figure 9 shows the lagged cross-correlation between glacier snout fluctuations and average summer temperature (from May to October) as a function of the lag. In the case of G69-99, we find slightly larger values of the cross-correlations and smaller lags than for G27-99. For G69-99, the index that shows the largest correlation corresponds to the shorter period of July-October ($r = 0.71$), with a smaller lag, τ = 7 y. However, this difference is not significant, as confirmed by the size of the error bars in Table 6.

< FIGURE 8 about here: average snout fluctuations and average summer temperature >

< FIGURE 9 about here: cross-correlation between snout fluctuations and temperature >

4. Construction of an empirical model of glacier response

4.1 General methodology

The simplest empirical model relating summer temperature and winter precipitation to glacier snout fluctuations assumes a linear dependence between the variables:

$$\overline{\delta x_i} = a_0 + a_T T_{i-\tau_T} + a_P P_{i-\tau_P} + \sigma_r W_i \qquad (3)$$

where $\overline{\delta x_i}$ is the standardized snout fluctuation in year i, averaged over all glaciers in the sample, $P_{i-\tau_P}$ and $T_{i-\tau_T}$ are the average standardized winter precipitation and summer temperature at years $i-\tau_P$ and $i-\tau_T$ respectively, τ_P and τ_T are the chosen lags for

precipitation and temperature, and we have omitted the indication of the duration of the period in the climatic variables. In this model, the homogeneous term a_0 measures the long-term trend. The coefficients a_T and a_p weight the temperature and precipitation dependencies, respectively. The last term is a noise term where σ_r^2 is the variance of the stochastic component and W_i is white noise with zero mean and unit variance.

To estimate the coefficients in the model we employ a standard least-squares method. In this context, in-sample predictions are equivalent to the least-square fit of the model to the data. A useful parameter to be monitored is the fraction of the variance of the data that is explained by the model:

$$R^2 = 1 - \frac{\sigma_r^2}{\sigma^2} \tag{4}$$

where σ^2 is the variance of the data.

4.2 Statistics of model residuals

A stochastic component is usually introduced in empirical regression models, to represent unresolved processes. Physically, the source of the stochastic term is related to measurement errors (mainly in the estimate of glacier snout position), and to processes that are not account for by the model. For example, the glacier terminus can undergo rapid changes due to break-ups and ice falls associated with motion on steep portions of the glacier bed, or with rapid melting of thin ice residuals. A stochastic component such as that included in equation (3) is a simplified way to describe these unresolved processes.

In the standard approach to stochastic modelling, the noise term W_i is required to have a Gaussian distribution with zero mean and unit variance, and to be δ–correlated in time, i.e., $\langle W_i W_k \rangle = \delta_{ik}$ where the brackets indicate ensemble average, $\delta = 1$ if $i = m$ and $\delta = 0$ if $i \neq m$ (Tong 1990). This is a "maximally random" version of the stochastic term that ensures that no significant statistical structure is left out of the model. In the following, we call "residuals", R_i, the differences between the data and the deterministic version of the model (3), i.e., $R_i = \overline{\delta x_i} - a_0 - a_T T_{i-\tau_T} - a_P P_{i-\tau_P}$. The analysis of the residuals provides a further test of the model: The residuals must be uncorrelated in time and have a Gaussian distribution if the model (3) is a

good descriptor of the dynamics, see e.g. Tong (1990) and Jacobson et al (2004) for a thorough discussion of residual evaluation. Gaussianity can be checked by looking at the higher moments of the residual's PDF and/or by a standard Kolmogorov-Smirnov test. Following Tong (1990), temporal decorrelation is assured at 95% confidence level, by requiring that no more than 5% of the autocorrelation values exceed the threshold $\pm\sqrt{1.96/N}$, where N is the dimension of the sample.

4.3 Robust estimate of model parameters and correlations

Randomization or bootstrap techniques are used to assess the significance of model parameter estimates (Tong, 1990; Jacobson et al, 2004). In practice, the randomization method works as follows. Suppose that a physical process is described by an empirical model containing a parameter, a, which links the output variable, y, to an input variable, x. In the simplest case, and the one considered here, we deal with a linear dependence, $y=ax+\sigma_r W$ where W is white noise. First, the value of a is estimated by the least-square fit of the x-y data. A large number of surrogate time series, $\{x^r\}$, is then generated, by random-shuffling the values of the input variable x. For each individual permutation, x^r, in the shuffled data set, the stochastic model is fitted to the x^r –y data and a value of the parameter, say a^r, is obtained (here, r labels the specific permutation of the input variable). The procedure is repeated a large number of times and a *shuffling* population of parameter values $\{a^r\}$ is obtained.

The expected value of a^r is zero. However, random fluctuations and finite statistics induce non-zero values of the parameters a^r. The distribution of the values of a^r allows for assessing whether the estimated value of a is significantly different from zero. Practically, this is done by estimating what fraction of the parameters values $\{a^r\}$, obtained from the shuffling population, is larger, in absolute value, than $|a|$ (note the use of a two-sided probability test). If this fraction is lower than a predetermined threshold (here set at 5%), then the parameter a is considered to be significantly different from zero at the selected confidence level (with our choice, at the 95% confidence level).

Error bars on the parameter estimates can be obtained by the jackknife method. Here, one estimates the parameter values from a random sub-sampling of the full data set (usually, half of

the total number of available data points) and repeats the estimates on a large number of different sub-samplings (i.e., random extractions from the data set). A distribution of parameter estimates is then obtained, which provides information on the average parameter value and on its variability due to random sub-samplings.

5. Reproduction of glacier snout fluctuations

5.1 Identification of the key variables

Our aim here is to build an empirical model for the ensemble response of large alpine glaciers to climate variability. To this end, we assume two simple constraints. First, the climatic variables must have a large lagged correlation with the snout fluctuations. Second, whatever is the mechanism that transmits the annual mass-balance signal through the glacier to its terminus, we ask that the maximum correlation lags τ_T and τ_P are close to each other. In deriving the empirical model, we shall concentrate on the period after 1950, for which both precipitation and temperature are available.

For winter precipitation, Table 5 indicates that the variable with the largest lagged correlation with snout fluctuations is $P_{(11–3)}$, with a time lag τ_P=10 y. All other precipitation variables have a significantly smaller correlation, and we thus opt for using this variable. For summer temperature, the variable with the largest correlation is $T_{(6–9)}$. However, in this case the correlation is maximum for a lag of 6 y, quite different from the lag obtained for precipitation. We note, however, that the variable $T_{(5–10)}$ has a correlation with the snout fluctuations which is statistically equivalent to that of $T_{(6–9)}$ (as indicated by the 95% confidence limits), and the correlation is maximized for a larger lag τ_T=8 y. We thus opt for using $T_{(5–10)}$ as a proxy for summer ablation and $P_{(11–3)}$ for winter accumulation. For the subset G69-99, the cross-correlation analysis suggests the use of $T_{(7–10)}$ for ablation and $P_{(11–3)}$ for accumulation. However, for consistency with the case of the subset G27-99 and owing to the small difference of the cross-correlation between $T_{(5–10)}$ and $T_{(7–10)}$, we opt for to use $T_{(5–10)}$ also for G69-99.

5.2 In-sample prediction

Model (3) is fitted to the average snout fluctuations in the G27-99 data set. Figure 10 shows the original snout fluctuation data together with the output produced by the deterministic part of the model (i.e., without the random noise term). The least-square fit uses the seasonal variables $T_{(5-10)}$ and $P_{(11-3)}$, shifted by their maximum correlation lag (of 8 and 10 years respectively). The empirical model correctly reproduces the decadal oscillation in the snout fluctuation signal and the variance explained by the model amounts to about 66%. We repeated the modelling exercise with other choices of the summer temperature variables, obtaining analogous results.

< FIGURE 10 about here: in-sample model prediction>

The values of the model parameter are reported in Table 7 for the G27-99 data set and in Table 8 for G69-99. These tables report also the probability that estimates from an ensemble of 1000 random re-orderings give parameter values that exceed, in absolute value sense, the value estimated from the original data, $P\left(\left|a^r\right| > |a|\right)$.

< TABLE 7 about here: results G27-99 >

< TABLE 8 about here: results G69-99 >

The results of the randomization test on the G27-99 data set indicate that the null hypothesis – that the values of the model parameters obtained from the least square fit are not significantly different from the value obtained with a random reordering of the data – must be rejected. The test is very robust for the parameters a_P and a_0. For the parameter a_T, the probability is at the threshold for rejection at the 95% confidence level. This is consistent with the fact that temperature records show a lower correlation with snout fluctuations than precipitation (figure 10). For G69-99, the estimated values of a_T and a_0 are not significantly different from zero, and the only parameter that is significantly different from zero is a_P. For this reason, we shall not consider further the empirical modelling of the G69-99 data set. It is interesting, however, that the significant dependence on winter precipitation in both data sets indicates that this variable is an important driver of glacier fluctuations.

The model residuals, R_i, are computed by subtracting the deterministic model hindcast from the data. As shown in figure 11(a), the distribution of the residuals is Gaussian at the 95% confidence level in a χ^2 sense for the G27-99 data set. The skewness of the distribution of the residuals is -0.38 with a 95% confidence threshold of -0.40. The kurtosis is -0.7 with a 95% confidence threshold of -0.8. Figure 11(b) shows that 90% of the values of the autocorrelation are below the threshold for white noise sequences (see the figure caption for further details). This confirms that a linear, empirical regressive process is able to capture at least some of the main processes responsible for the average response of glacier snout fluctuations to climate variability.

< FIGURE 11 about here: residuals for G27-99>

6. Out-of-sample prediction of glacier response

An important test of a model concerns its capability of forecasting glacier fluctuations from the knowledge of (measured or forecasted) climatic indices beyond the temporal range used to train the model. In the case of out-of-sample predictions, the model parameters must be determined, by means of least-square fitting, from a given portion of the data set, and the model should then be used to forecast the glacier response to temperature and precipitation variations in the data portion other than that used to estimate the model parameters. Clearly, good out-of-sample predictions are harder to obtain but they are much more useful than in-sample predictions, as they allows for true forecasting.

To verify the ability of the linear model to perform out-of-sample predictions, we estimate the model parameters from the first portion of the available data (which we call the training period) and use the parameter estimates obtained in this way to forecast glacier snout fluctuations from the knowledge of temperature and precipitation in the second half of the time series (which is then used as the verification period). Figure 12 shows the original data with the result of the out-

of-sample predictions for the period 1980-1999. The empirical linear model (3) has been trained on the years 1961-1980 (corresponding to temperature measured in the period 1953-1972 and precipitation in the period 1951-1970). The empirical model is then advanced in time, with the inclusion of a white-noise stochastic component with variance equal to that of the residuals of the model. The procedure is repeated 1000 times; figure 12 shows the average of the ensemble of realizations together with the 5th and the 95th percentiles on the ensemble of out-of-sample predictions. The observed data fall inside the ensemble prediction band defined by the 5th and 95th percentiles.

< FIGURE 12 about here: out-of-sample prediction of snout fluctuations>

An interesting point concerns the performance of the empirical model when different training sets are used. The entire data set contains $N = 39$ yearly data points, from 1961 to 1997. In the following, we train the model on the first N_t years and we then integrate forward in time for $N - N_t + \tau_T$ years, so that all the needed temperature and precipitation indices are available. Figure 13 shows the results for different values of N_t. Each curve in the figure is obtained as an average over 10000 realizations of the model forecasts. The random component of the empirical model has zero mean and variance estimated from the residuals calculated on the training set.

Unlike in previous figures, the results reported in figure 13 have been converted to dimensional units and refer to the average snout position rather than to snout fluctuation, to provide an illustration of the expected mean retreat of large alpine glaciers. The standardized annual mean snout variation $\overline{\delta x_i}$ has been converted to dimensional units by averaging over the ensemble of glaciers the individual mean snout fluctuations and their r.m.s. deviations, i.e. $\overline{\delta X_i} = \overline{\delta X} + \sigma \overline{\delta x_i}$ where $\overline{\delta X} = \left\langle \overline{\delta X^j} \right\rangle$ and $\sigma = \left\langle \sigma^j \right\rangle$. The mean snout position is then obtained as $\overline{X_i} = \sum_{k=1}^{i} \overline{\delta X_k}$.

< FIGURE 13 about here: out-of-sample forecasts for different training sets >

Figure 13 confirms that when the training set is long enough, the linear model is able to quantitatively predict the average snout position. In the case of the forecasts starting in 1968 and

1972, corresponding to short training sets of duration N_t = 7 y and N_t = 13 y, the performance of the model is poor, featuring a considerable spread and large deviations from the observations. Instead, in the case of longer training sets, the spread of the model forecasts decreases and the agreement between the forecasts and the observations is very good.

5. Discussion and conclusions

We have analyzed the time series of snout fluctuations of a large ensemble of glaciers in the Western Italian Alps, focussing on the behaviour of nine large glaciers that were monitored for several decades. Most of the glaciers display an overall recessional trend, which is faster in the first half of the 20th Century. In the second half of the Century, these glaciers are characterized by a slower retreat and by short episodes of snout advance. In addition, the overall recession is modulated by oscillations on a decadal time-scale, as shown in Figures 3, 4 and 5.

The results of the analysis indicate that the ensemble-averaged yearly snout fluctuations are significantly correlated with the summer temperature and winter precipitation signals, which can be adopted as proxies for the full climatic conditions and for the overall glacier mass balance. A simple empirical, regressive lagged-linear model based on these variables explains about 66% of the variance of the average snout fluctuation signal.

Since the climatic variables used in the empirical model are standardized, the quantitative values of the model parameters, reported in Table 7, give an estimate of the relative importance of summer temperatures and winter precipitation in characterizing the snout fluctuations. For the long G27-99 data set, the weight of winter precipitation is almost twice as large as that of summer temperature. Thus, winter precipitation rates seem to drive the snout fluctuations more effectively than summer temperatures. This also suggests that the slow-down of glacier retreat in the second half of the 20th Century might result from the occurrence of a warmer/wetter climate in Alpine areas. Other occurrences of this phenomenon have been reported elsewhere (Mayo and March, 1990).

The linear empirical model has been shown to produce reliable out-of-sample predictions of glacier response to climate variability. In this approach, we determined the model parameters only from the first portion of the data set and we used the model determined so far to predict glacier snout fluctuations in the second part of the data set, using as input the measured time series of summer temperature and winter precipitation. To test the performance of the procedure, the model output is then compared to the measured snout fluctuation data available in the second part of the record, as shown in Figures 12 and 13. The results of the comparison indicate that the simple model (3) is capable of correctly forecasting, out-of-sample, glacier snout fluctuations from the knowledge of proxy climatic variables.

The satisfactory performance of the out-of-sample forecast provided by the empirical model introduced here suggests interesting developments, when used in combination with climate change predictions (e.g., Oerlemans et al., 1998; Van de Wal and Wild, 2001). The statistical robustness of the results obtained in this work indicates that, when reliable and high-resolution simulations of future climate change scenarios at regional scale over Europe will become available, the empirical approach discussed here can provide quantitative estimates of the impact of climate change on average glacier snout fluctuations in the Alps.

Acknowledgements

This work was supported by a grant of ARPA – Piemonte. We acknowledge useful discussions with J. Oerlemans and with L. Mercalli.

Appendix 1. Estimate of the seasonal variables.

Let p_{im}^q be the monthly mean precipitation rate at the q-th station in year i and month m. The standardized monthly precipitation rate is defined as:

$$\pi_{im}^q = \frac{p_{im}^q - \overline{p_m^q}}{\sigma_m^q} \quad , \tag{A1}$$

where

$$\overline{p_m^q} = \frac{1}{N_m^q} \sum_i p_{im}^q$$

is the average and

$$\sigma_m^q = \sqrt{\frac{\sum_i \left(p_{im}^q - \overline{p_m^q}\right)^2}{N_m^q}}$$

is the r.m.s. value. Here N_m^q is the number of data values available for the q-th station and the m-th month. The seasonal value is then computed as

$$P_{i(n-m)} = \frac{1}{N_{months}} \sum_{j=m}^{n} \left(\frac{1}{N_{stations}} \sum_{q=1}^{N_{stations}} \pi_{ij}^q \right) \tag{A2}$$

where N_{months} is the number of months included in the definition of the season and $N_{stations}$ is the number of available weather stations.

References

Bohm R, Auer I, Brunetti M, Maugeri M, Nanni T, Schoner W. 2001. Regional temperature variability in the European Alps: 1760-1998 from homogeneized instrumental time series. *International Journal of Climatology* **21**: 1779-1801.

Braithwaithe RJ, Zhang Y. 1999. Relationships between interannual variability of glacier mass balance and climate. *J. Glaciology* **45**: 456-462.

Clague JJ, Evans SG. 2000. A review of catastrophic drainage of moraine-dammed lakes in British Columbia. *Quaternary Sci. Reviews* **19**: 1763-1783.

Chinn TJ. 1996. New Zealand glacier responses to climate change of the past century. *New Zeal. J. Geol. Geophys.* **39**: 415-428.

Ciccarelli N, von Hardenberg J, Provenzale A, Ronchi C, Vargiu A. 2006. An analysis of climate variability during the second half of the 20th Century in North-Western Italy. Proceedings of the General Assembly of the *European Geosciences Union*, Vienna, 2-7 April 2006, EGU06-A-07104.

Giorgi F, Bi X, Pal J, 2004. Mean, interannual variability and trends in a regional climate change experiment over Europe. II: climate change scenarios (2071–2100). *Clim. Dyn.,* **23**: 839-858.

Greene AM, Broecker WS, Rind D. 1999. Swiss glacier recession since the Little Ice Age: Reconciliation with climate records. *Geophys. Res. Lett.* **26**: 1909-1912.

Haeberli W. 1995. Glacier fluctuations and climate change detection. *Geogr. Fis. Dinam. Quat*. **18**: 191-199.

Harper J. 1993. Glacier Terminus Fluctuations on Mount Baker, Washington, U.S.A., 1940-1990, and Climatic Variations. *Arctic Alpine Res*. **25**: 332-340.

Harrison S, Winchester V. 2000. Nineteenth- and twentieth-century glacier fluctuations and climatic implications in the Arco and Colonia valleys, Hielo Patagonico Norte, Chile. *Arct. Antarct. Alp. Res* **32**: 55-63.

Holmlund P, Fuenzalida H. 1995. Anomalous glacier responses to 20th century climatic changes in Darwin Cordillera, southern Chile. *J. Glaciology* **41**: 465-473.

Jacobson AR, Provenzale A, von Hardenberg A, Bassano B, Festa-Bianchet M. 2004. Climate forcing and density dependence in a mountain ungulate population. *Ecology* **85**: 1598-1610.

Kaser G. 1999. A review of modern fluctuations of tropical glaciers. *Global Planetary Change* **22**: 93-103.

Kaser G, Osmanston H. 2001. *Tropical Glaciers*. Cambridge University Press: Cambridge.

Kaser G, Hardy DR, Molg T, Bradley RS, Hyera TM. 2004. *International J. Climatology* **24**: 329-339.

Kruss P. 1984. Terminus response of Lewis glacier, Mount Kenya, Kenya, to sinusoidal net-balance forcing. *J. Glaciology* **30**: 212-217.

Laumann T, Reeh N. 1993. Sensitivity to climate change of the mass balance of glaciers in southern Norway. *J. Glaciology* **39**: 656-665.

Letreguilly A. 1988. Relation between the mass balance of western Canadian mountain glaciers and meteorological data. *J. Glaciology* **34**: 11-18.

Mayo LR, March RS. 1990. Air temperature and precipitation at Wolverine glacier, Alaska; glacier growth in a warmer, wetter climate. *Ann. of Glaciol.* **14**: 191-194.

Nesje A. 1989. Glacier front variations of outlet glaciers from Jostedalsbreen and climate in the Jostedalsbre region of western Norway in the period 1901-80. *Norsk Geogr. Tidssk.* **43**: 3-17.

Nesje A, Dahl SO. 2000. *Glaciers and Environmental Change*. Arnold Publishers: London.

Oerlemans J, Anderson B, Hubbard A, Huybrechts P, Johannesson T, Knap WH, Schmeits M, Stroeven AP, Van de Wal RSW, Wallinga J, Zuo Z. 1998. Modelling the response of glaciers to climate warming. *Climate Dynamics* **14**: 267-274.

Oerlemans J, Reichert BK. 2000. Relating glacier mass balance to meteorological data by using a seasonal sensitivity characteristic. *J. Glaciology* **46**: 1-6.

Oerlemans J. 2001. *Glaciers and Climate Change*. Balkema Publishers: Lisse.

Paterson WSB. 1994. *The Physics of Glaciers*. Pergamon: New York.

Posamentier HW. 1977. A new climatic model for glacier behaviour of the Austrian Alps. *J. Glaciology* **18**: 57-65.

Pelfini M. 1994. Equilibrium line altitude (ELA) variations recorded by Ortles-Cevedale glaciers (Lombardy, Italy) from the Little Ice Age to present. *Geogr. Fis. Dinam. Quat.* **17**: 197-206.

Regione Piemonte. 1998. Distribuzione regionale di piogge e temperature. *Collana studi climatologici in Piemonte,* **1**.

Sturm M, Hall DK, Benson CS, Field WO. 1991. Non-climatic control of glacier-terminus fluctuations in the Wrangell and Chugach Mountains, Alaska, U.S.A. *J. Glaciology* **37**: 348-356.

Theakstone H. 1990. Twentieth-century glacier change at Svartisen, Norway: the influence of climate, glacier geometry and glacier dynamics. *Annals of Glaciology* **14**: 283-287.

Tong H. 1990. *Nonlinear time series: a dynamical system approach*. Oxford Univ. Press: Oxford.

Van de Wal RSW, Wild M. 2001. Modelling the response of glaciers to climate change by applying volume-area scaling in combination with a high resolution GCM. *Climate Dynamics* **18**: 359-366.

Vanuzzo C. 2001. The glacier retreat in Valle d'Aosta (western italian Alps) from the Little Ice Age to the second half of the 20th century: linear, areal volumetric and equilibrium line altitude changes. *Geogr. Fis. Dinam. Quat.* **24**: 99-113.

Vincent C. 2002. Influence of climate change over the 20th Century on four French glacier mass balances. *J. Geophys. Res*. **107 D**: 000832.

Yafeng S, Jiawen R. 1990. Glacier recession and lake shrinkage indicating a climatic warming and dry trend in central Asia. *Ann. Glaciology* **14**: 261-265.

Glacier	Lat	Lon	L [m]	Slope [deg]	Asp [deg]	N	$\overline{\delta X^j}$ [m]	σ^j [m]
Belvedere	45°57’	4°34’	6000	10	45	43	-11.7	14.4
Cherillon	45°57’	4°50’	1800	19	90	42	-3.5	9.6
Lex Blanche	45°47’	5°38’	3500	24	135	35	-0.8	16.2
Lys	45°40’	4°37’	5300	20	270	80	-6.0	15.4
Moncorve	45°30’	5°12’	2125	20	270	25	-9.2	11.7
Piccolo di Verra	45°50’	4°41’	3200	21	270	34	-11.7	14.8
Pre de Bar	45°54’	5°24’	3500	23	135	57	-3.0	13.8
Toula	45°50’	5°31’	1500	24	135	18	2.9	10.4
Valtournanche	45°54’	4°45’	2000	19	270	51	-11.7	12.1

Table 1. Characteristics of the glaciers in the data set G27-99. For each glacier, the columns report, from left to right: latitude, longitude, nominal glacier length, average slope, aspect (orientation), number of sampled years, average snout fluctuation and standard deviation (r.m.s. fluctuation) of the snout variations.

Glacier	Lat	Lon	L [m]	Slope [deg]	Asp [deg]	N	$\overline{\delta X^j}$ [m]	σ^j [m]
Clapier	44°07’	5°02’	360	16	45	25	-1.0	2.7
Peirabroc	44°07’	5°02’	154	13	90	29	-1.2	1.8
Galambra	45°06’	5°35’	850	20	45	8	-4.7	10.7
Fourneaux	45°07’	5°36’	600	15	315	7	-1.1	14.1
Agnello	45°09’	5°33’	900	20	45	9	-5.3	10.7
Rocciamelone	45°12’	5°22’	1000	1	45	5	-0.4	1.8
Pera Ciaval	45°14’	5°19’	250	1	135	3	-2.2	11.6
Bessanese	45°18’	5°19’	2300	15	135	12	-6.1	11.8
Ciamarella	45°19’	5°19’	900	18	90	13	-1.4	5.6
Martellot	45°22’	5°16’	800	38	135	12	-1.8	6.8
Capra	45°26’	5°20’	950	16	0	5	-7.2	4.0
Basei	45°28’	5°20’	900	30	0	14	-1.0	1.5
Breuil	45°29’	5°h1’	1000	25	90	9	-3.7	7.2
Ciardoney	45°31’	5°03’	1950	8	90	12	-1.3	6.9
Sengie Setten	45°32’	5°03’	1050	32	45	6	-5.5	10.5
Money	45°31’	5°07’	2600	25	45	8	-7.8	10.4
Lauson	45°34’	5°10’	1000	15	45	11	-3.6	3.7
Vaudaletta	45°31’	5°19’	400	20	315	5	-10.2	15.2
Lavassey	45°28’	5°20’	1950	22	135	14	-7.6	8.1
Fond Orientale	45°28’	5°21’	2150	15	315	13	-3.9	10.5
Soches-Tsantel	45°29’	5°23’	3500	12	45	14	-5.8	6.1
Goletta	45°29’	5°23’	2375	18	0	8	-3.4	4.0
Gliairetta Vaud	45°30’	5°26’	3575	9	90	6	-7.5	12.0
Rutor	45°30’	5°27’	8375	6	315	23	-2.7	5.3
Chavannes	45°44’	5°38’	1300	15	90	10	-7.0	6.5
Estellette	45°46’	5°38’	1250	24	135	6	5.5	7.4
Netscho	45°49’	4°35’	300	23	315	11	-2.2	2.5
Piode	45°54’	4°34’	2250	31	135	17	-7.9	17.8
Nord Andolla	46°05’	4°24’	600	30	135	14	-4.8	7.1
Osand Sett.	46°24’	4°07’	4330	7	90	19	-4.0	7.0

Maledia	44°07’	5°03’	130	18	45	26	-1.5	3.2
Muraion	44°07’	5°03’	230	16	45	22	-0.9	3.3
Gelas	44°07’	5°03’	170	18	0	21	-0.7	2.5
Tza de Tzan	45°58’	4°53’	5900	15	90	10	-8.4	15.8
Grande di Verra	45°55’	4°42’	5250	18	90	26	-11.6	7.8
Indren	45°53’	4°35’	2500	21	90	14	-5.6	4.4

Table 2. Characteristics of the glaciers in the subset G69-99. Same details as in table 1.

Data set	N	ν	χ^2	χ_0^2	d	d_0
G69-99	458	22	54	32	0.077	0.063
G27-99	394	22	66	32	0.089	0.071
G27-99(limited)	356	19	26	30	0.047	0.072

Table 3. Results of the χ^2 and K-S tests of the Gaussianity of the distribution of glacier snout fluctuations. N is the total number of data points, ν is the number of degrees of freedom for the χ^2 test, d is the *distance* of the distribution from a Gaussian, according to the K-S test. The values χ_0^2 and d_0 are the critical values above which the hypothesis that the data have a Gaussian distribution must be rejected.

Months	G27-99			G69-99		
	r	δr	τ [years]	r	δr	τ [years]
$P_{(11-3)}$	0.45	0.17	9	0.58	0.14	9
$P_{(11-2)}$	0.41	0.18	9	0.48	0.12	10
$P_{(12-3)}$	0.46	0.17	9	0.53	0.20	9
$P_{(1-3)}$	0.47	0.17	6	0.61	0.19	8
$P_{(1-3)}$	0.57	0.11	5	0.62	0.19	9

Table 4. Lagged cross-correlations between winter precipitation and average snout fluctuations for the G27-99 and G69-99 data sets.

Months	1900-1950			1950-2000		
	r	δr	τ [years]	r	δr	τ [years]
$P_{(11-3)}$	0.63	0.24	6	0.78	0.08	10
$P_{(11-2)}$	0.57	0.26	6	0.57	0.12	11
$P_{(12-3)}$	0.64	0.24	6	0.63	0.13	9
$P_{(1-3)}$	0.58	0.26	6	0.52	0.17	9
$P_{(1-3)}$	0.66	0.24	5	0.64	0.15	9

Table 5. Lagged cross-correlations between winter precipitation and average snout fluctuations for the data set G27-99, during the two halves of the XX century.

Months	G27-99			G69-99		
	r	δr	τ [years]	r	δr	τ [years]
$T_{(5-9)}$	-0.62	0.12	6	-0.63	0.11	6
$T_{(5-10)}$	-0.63	0.12	8	-0.69	0.09	7
$T_{(6-9)}$	-0.66	0.14	6	-0.66	0.10	7
$T_{(6-10)}$	-0.54	0.15	9	-0.68	0.10	8
$T_{(7-9)}$	-0.61	0.12	8	-0.70	0.09	7
$T_{(7-9)}$	-0.63	0.13	8	-0.71	0.08	7

Table 6. Lagged cross-correlations between summer temperatures and average snout fluctuations for the data sets G27-99 and G69-99.

Parameter	Value	Jackknife	$P\left(\left\|a^r\right\| > \|a\|\right)$
a_T	-0.61	-0.62±0.18	0.05
a_P	1.11	1.10±0.22	0.0003
a_0	0.29	0.29±0.04	0.

Table 7. Parameter estimates and probability of the null hypothesis that the parameter value is null, for the G27-99 data sets. The first column identifies the parameter, the second column reports the value obtained by fitting the linear model to the whole data set, the third column reports the average value of the parameter and the r.m.s. fluctuation (1σ) obtained by a jackknife procedure where the parameter is estimated from half of the data set, and the fourth column reports the probability that the parameter estimate from a random reordering of the data is larger, in absolute value, than the original parameter. Probabilities and jackknife estimates have been obtained from a total of 1000 random re-orderings (for the bootstrap) or sub-samplings (for the jackknife) of the time series.

Parameter	Fit	Jacknife	$P\left(\left\|a^r\right\| > \|a\|\right)$
a_T	-0.48	-0.50±0.16	0.15
a_P	0.60	0.60±0.18	0.02
a_0	0.11	0.10±0.03	0.93

Table 8. Same as in Table 7 but for the data set G69-99.

Figure 1. Picture of the Pre de Bar glacier (Val d'Aosta, Italy) in summer 2001. The lower red line marks the glacier snout. The upper red line provides a qualitative illustration of the Equilibrium Line that separates the region where accumulation dominates from the region where ablation dominates. The black arrow qualitatively indicates the ice flow. Note the stream formed by the melting ice below the snout.

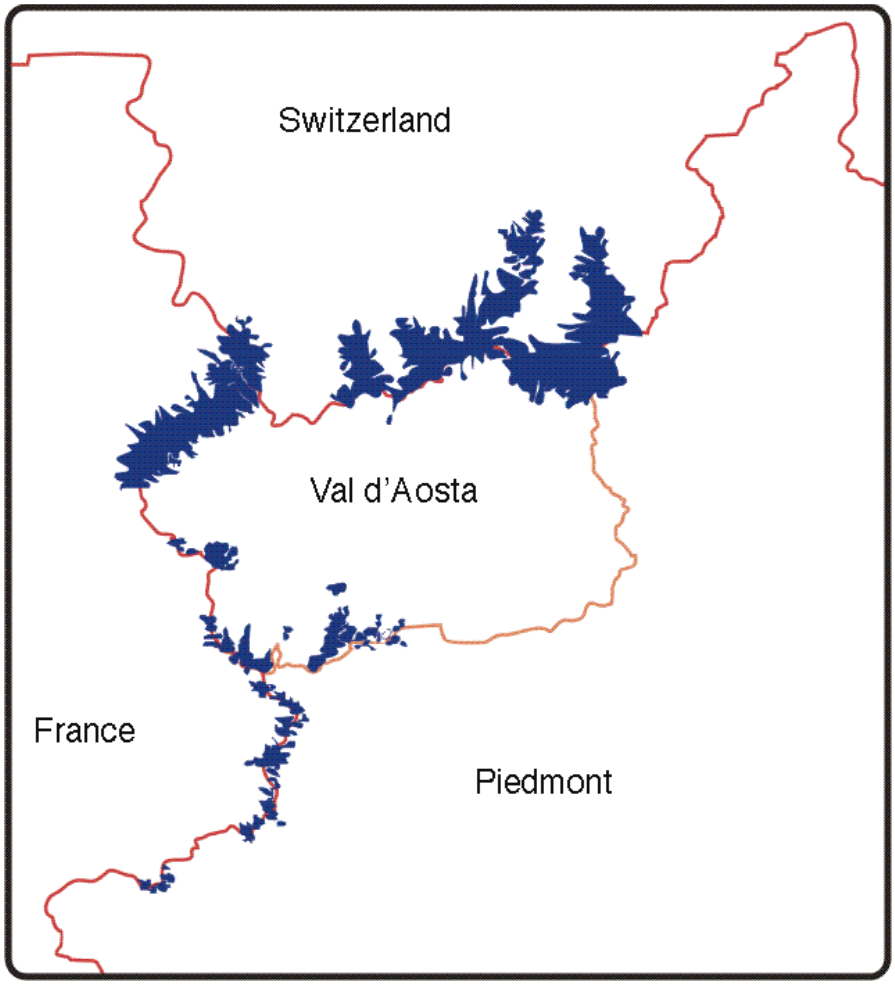

Figure 2. Schematic map of the study area (North-Western Italy). The locations where mountain glaciers are found are indicated in blue.

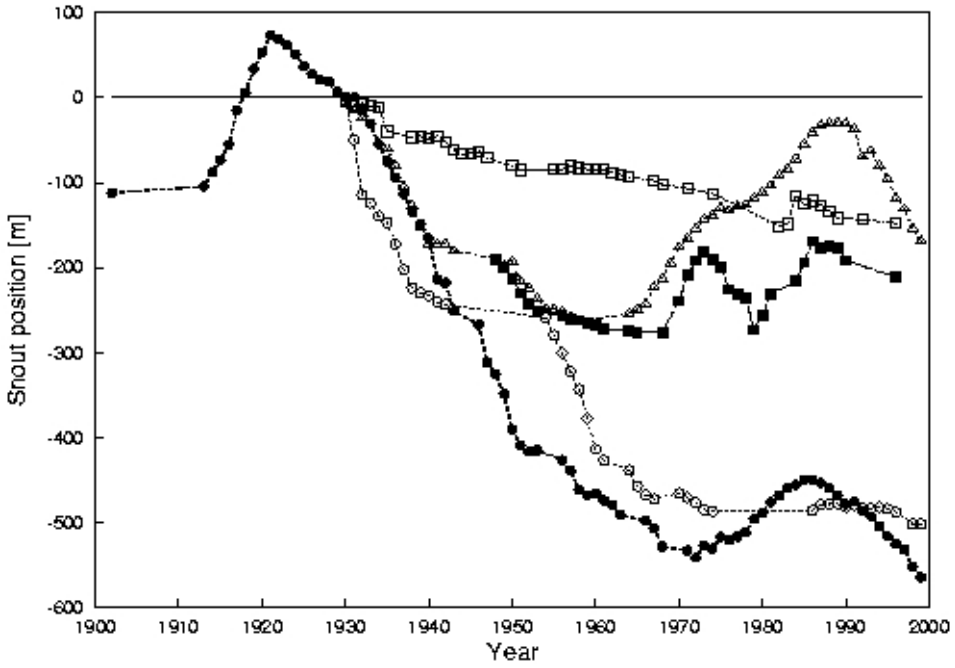

Figure 3. Annual snout positions, X_i^j, for five representative glaciers in the data set G27-99. We arbitrarily set the origin of the distance axis at the glaciers' position in 1930, when several glaciers started to be monitored.

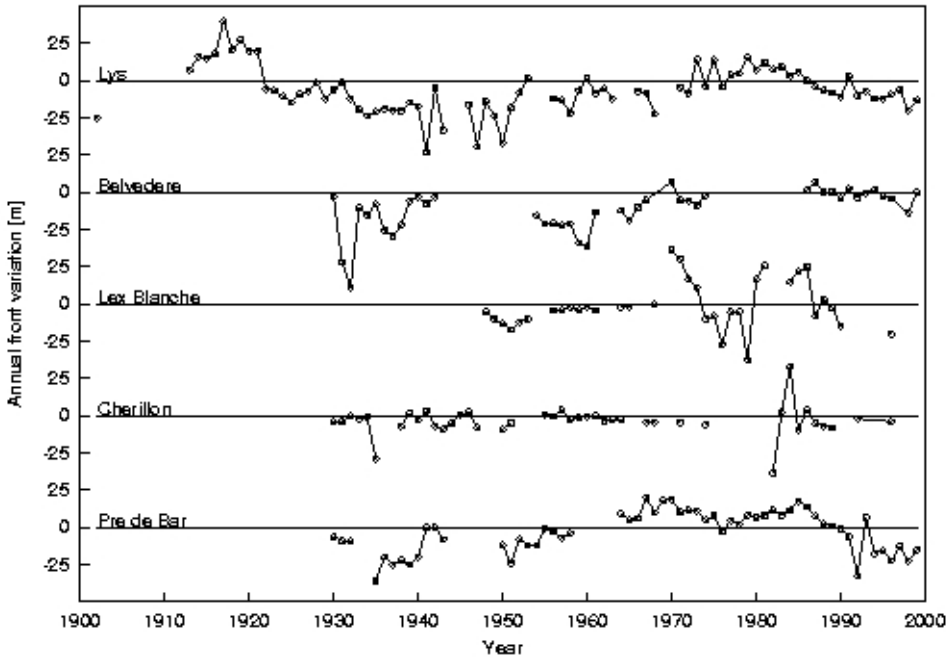

Figure 4. Annual snout fluctuations, δX_t^j, for the same five glaciers shown in figure 3.

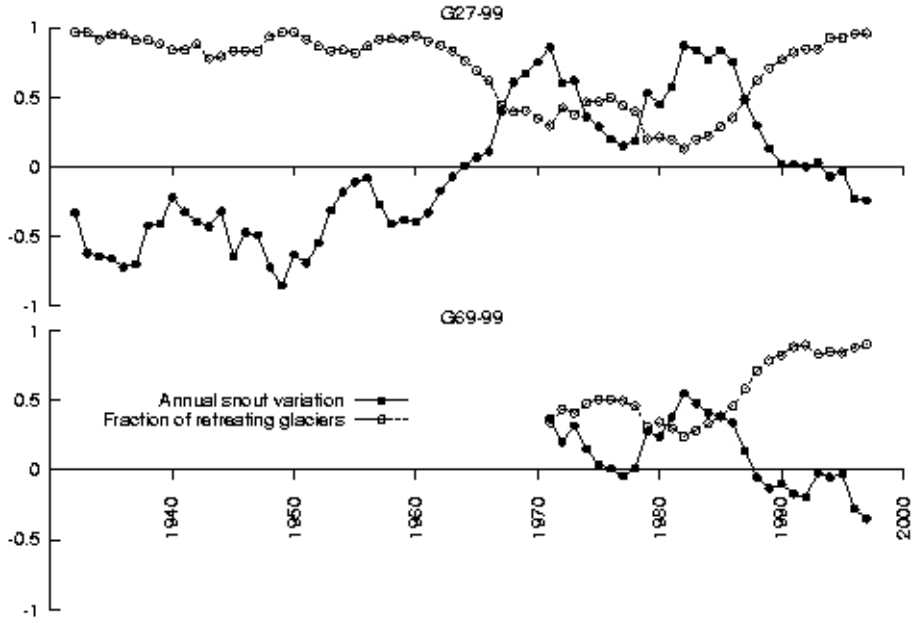

Figure 5. Average annual snout variation (solid points) and fraction of retreating glaciers (hollow points) for the datasets G27-99 (upper panel) and G69-99 (lower panel).

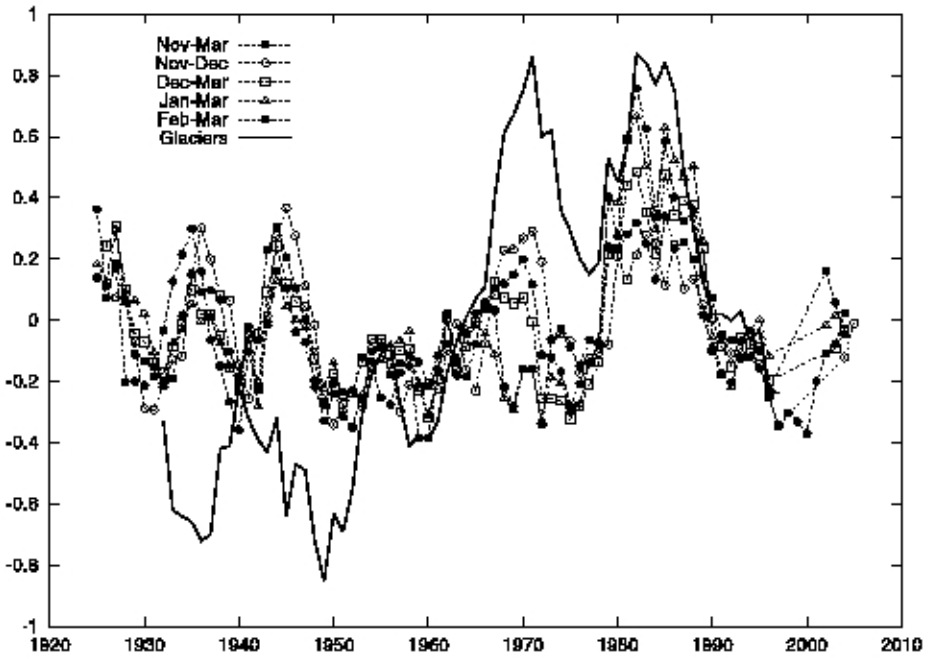

Figure 6. Average glacier snout fluctuations (solid line) and winter precipitation (defined in different periods as indicated in the legend). Winter precipitation has been displaced by the time lag that gives the maximum cross-correlation with the snout fluctuations.

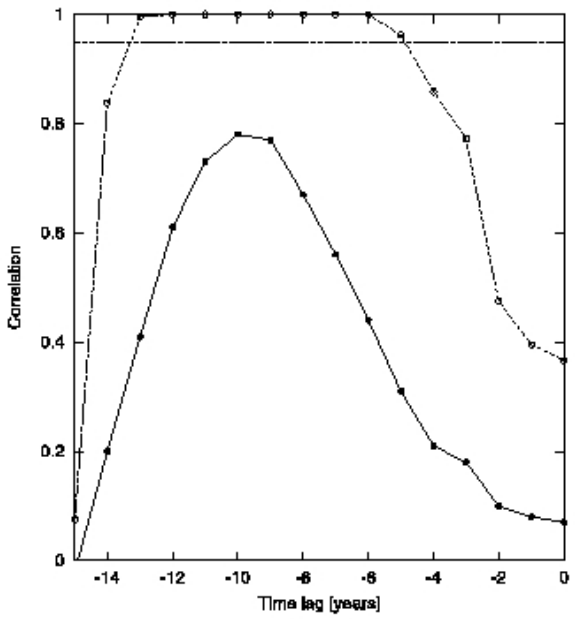

Figure 7. Solid curve: Lagged cross-correlation between average snout fluctuations and winter precipitation from November to March as a function of the time lag in years, for the G27-99 data set in the period 1950-1999. Dashed curve: Probability that the cross-correlation is different from zero, as obtained from random re-orderings of the data set. The upper horizontal line indicates the level of 95% significance.

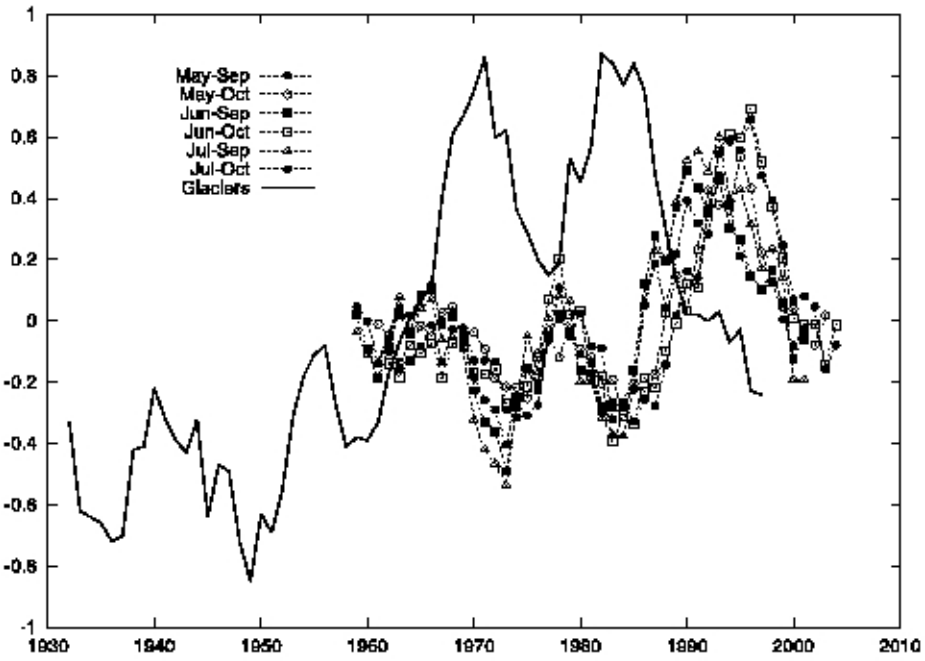

Figure 8. Average glacier snout fluctuations (solid line) and summer temperature (defined in different periods as indicated in the legend). Summer temperature has been displaced by the time lag that gives the maximum cross-correlation with the snout fluctuations.

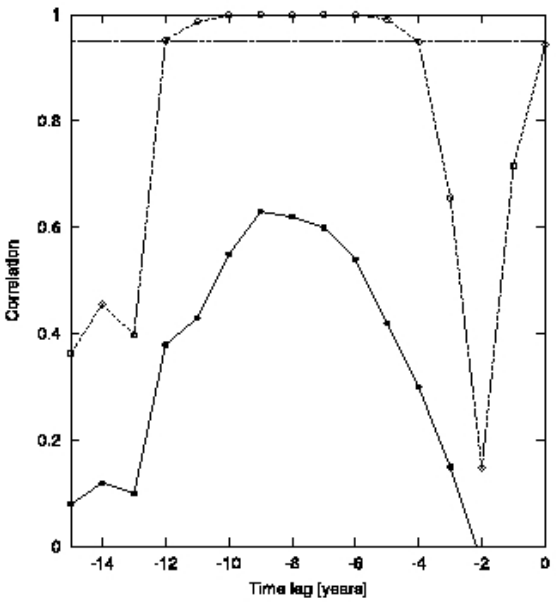

Figure 9: Lagged cross-correlation between average snout fluctuations and average summer temperature from May to October for the G27-99 data set. Dashed curve: Probability that the cross-correlation is different from zero, as obtained from random re-orderings of the data set. The upper horizontal line indicates the level of 95% significance.

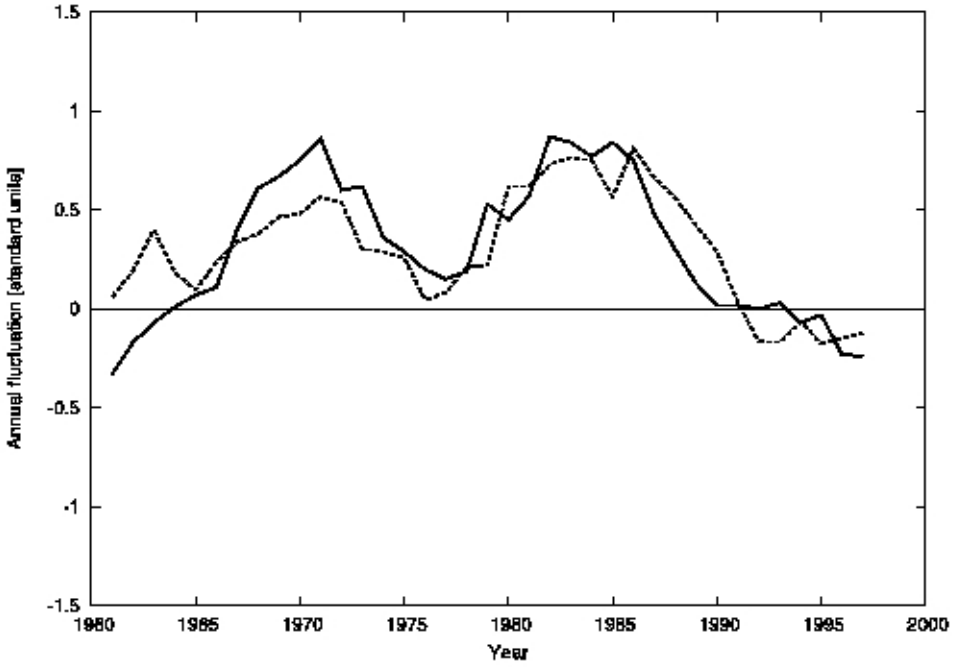

Figure 10. Dashed curve: In-sample deterministic prediction for the G27-99 averaged annual snout variation with the empirical lagged-linear model. The solid curve is the averaged snout variation derived from the data; the dashed line is the output of the deterministic part of the model. The explained variance is 66%.

(a)

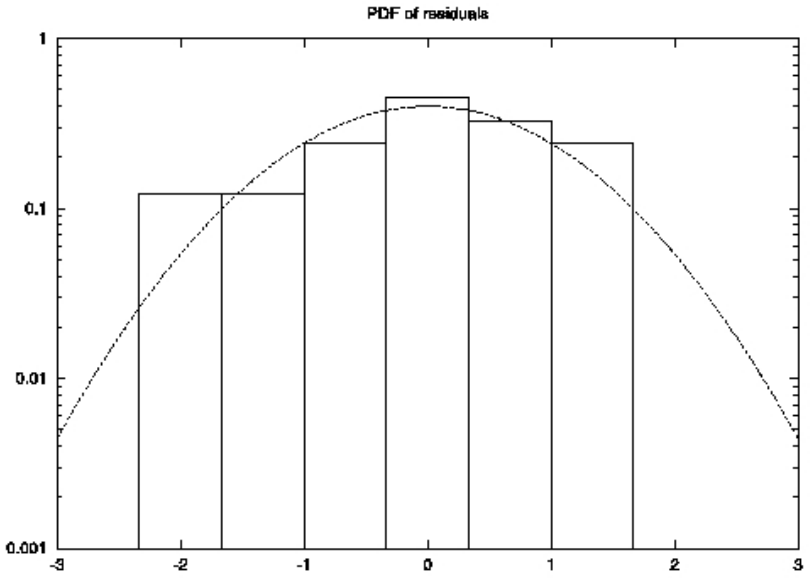

(b)

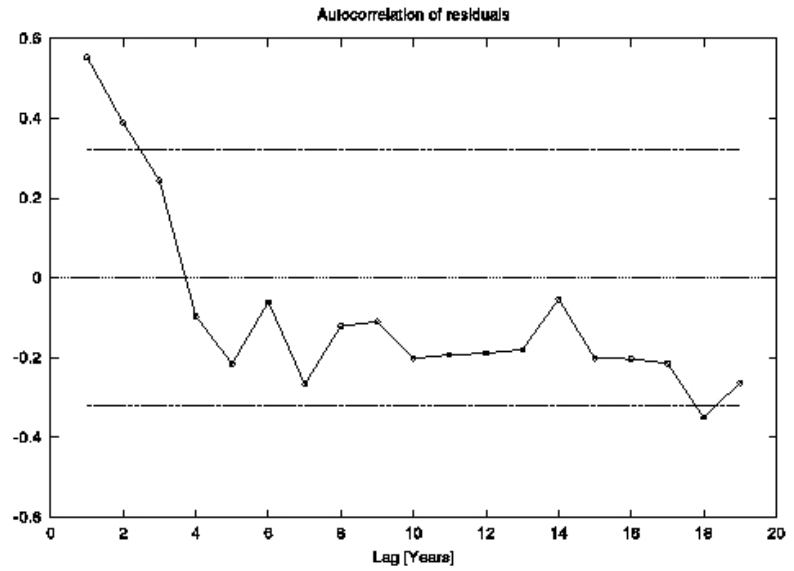

Figure 11. Panel a: Distribution of the residuals of the model trained on G27-99. The superposed dashed line represents a Gaussian distribution. The distribution of the residuals is Gaussian at the 95% confidence level in the χ^2 sense. The skewness of the distribution of the residuals is -0.38 with a 95% confidence threshold of -0.40. The kurtosis is -0.7 with a 95% confidence threshold of -0.8. Panel (b) shows the autocorrelation of the residuals. The dashed lines are the thresholds required for rejecting the hypothesis that the residuals are correlated. More than 90% of the values do not exceed the threshold. Positive autocorrelation for lag less than 5 years is expected because of the 5-y running mean applied to the data.

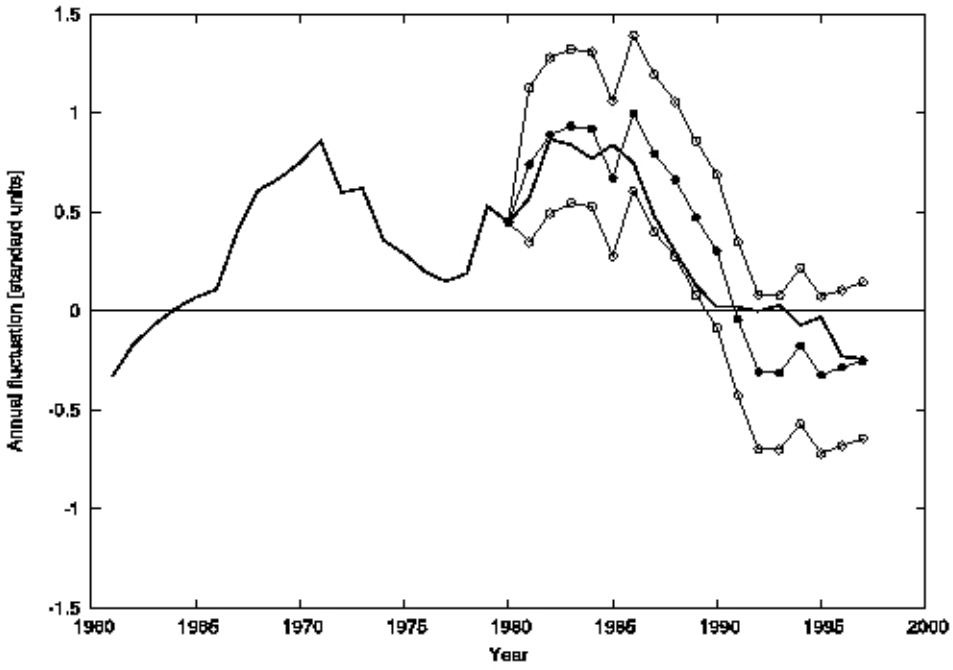

Figure 12. Out-of-sample prediction of the average annual snout variation for the dataset G27-99. The solid line represents the data. The solid points are the average of 1000 different out-of-sample predictions obtained by training the stochastic linear model on the first 20 years of data. The hollow points represent the 5-th and 95-th percentiles of 1000 different forecasts.

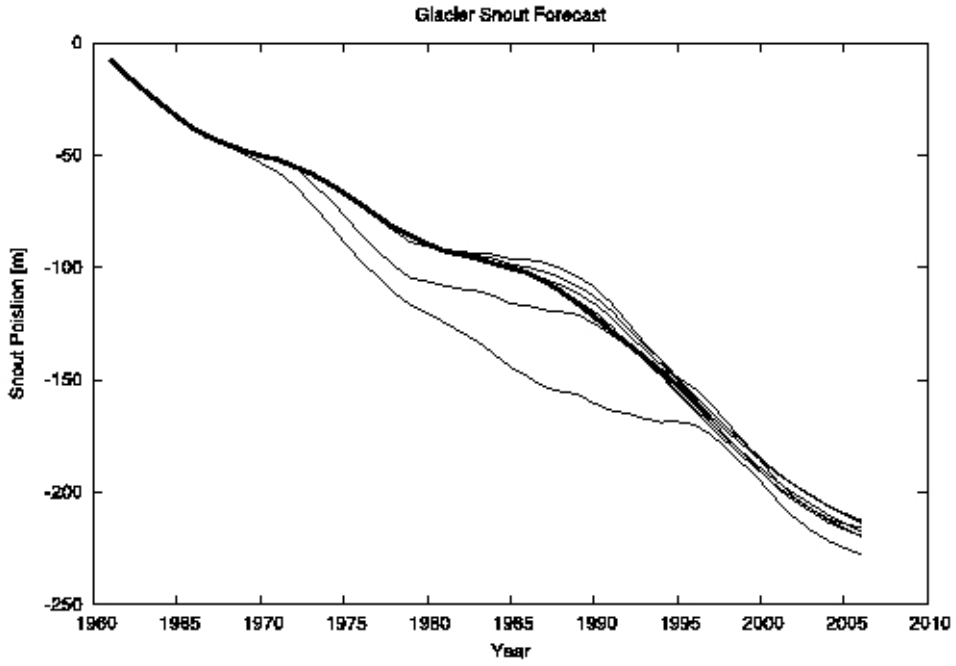

Figure 13. Cumulated average snout variation for the dataset G27-99. The thick line is the snout variation obtained from data. The thin lines are the averages over 10000 out-of-sample forecasts obtained from the linear stochastic model with different training subsets. The forecasts reported in the figure start in 1968, 1972, 1976, 1980, 1984, 1988, 1992 and 1996. The durations of the corresponding training sets are 7, 13, 17, 21, 25, 29, 33 and 37 years.